Traffic 2006; 7: 337–353
Blackwell Munksgaard

doi: 10.1111/j.1600-0854.2006.00387.x

Two Di-Leucine Motifs Regulate Trafficking of Mucolipin-1 to Lysosomes

Silvia Vergarajauregui and Rosa Puertollano*

Laboratory of Cell Biology, National Heart, Lung, and Blood Institute, National Institutes of Health, Bethesda, MD 20892, USA
** Corresponding author: Rosa Puertollano, puertolr@mail.nih.gov*

Mutations in the mucolipin-1 gene have been linked to mucolipidosis type IV, a lysosomal storage disorder characterized by severe neurological and ophthalmologic abnormalities. Mucolipin-1 is a membrane protein containing six putative transmembrane domains with both its N- and C-termini localized facing the cytosol. To gain information on the sorting motifs that mediate the trafficking of this protein to lysosomes, we have generated chimeras in which the N- and C- terminal tail portions of mucolipin-1 were fused to a reporter gene. In this article, we report the identification of two separate di-leucine-type motifs that co-operate to regulate the transport of mucolipin-1 to lysosomes. One di-leucine motif is positioned at the N-terminal cytosolic tail and mediates direct transport to lysosomes, whereas the other di-leucine motif is found at the C-terminal tail and functions as an adaptor protein 2-dependent internalization motif. We have also found that the C-terminal tail of mucolipin-1 is palmitoylated and that this modification might regulate the efficiency of endocytosis. Finally, the mutagenesis of both di-leucine motifs abrogated lysosomal accumulation and resulted in cell-surface redistribution of mucolipin-1. Taken together, these results reveal novel information regarding the motifs that regulate mucolipin-1 trafficking and suggest a role for palmitoylation in protein sorting.

Key words: di-leucine, lysosomes, MLIV, mucolipin-1, sorting

Received 8 September 2005, revised and accepted for publication 5 December 2005, published on-line 9 January 2006

OnlineOpen: This article is available free online at www.blackwell-synergy.com

Mucolipidosis type IV (MLIV) is an autosomal recessive neurodegenerative lysosomal storage disorder characterized by psychomotor retardation and visual impairment (1). Symptoms usually appear in the first year of life and include progressive mental and motor deterioration, corneal clouding, retinal degeneration and strabismus (2,3). This disorder is found at a relative high frequency among Ashkenazi Jews, with 1/100 of the population estimated to be a genetic carrier (4). The analysis of fibroblasts from MLIV patients by electron microscopy revealed the presence of enlarged vacuolar structures that accumulate phospholipids, mucopolysaccharides and gangliosides and display a higher pH than normal lysosomes (5–8). In contrast with most lysosomal storage disorders, lysosomal hydrolases in MLIV are normal and the accumulation of the observed material seems to result from defects in transport along the lysosomal pathway (9,10).

Linkage analysis carried out in 13 Ashkenazi Jewish families mapped the MLIV locus to chromosome 19p13.3-p13.2 (11) and allowed the identification of MCOLN1 as the gene responsible for the disease (12–14). MCOLN1 encodes a 580-amino acid protein named mucolipin-1 with a predicted molecular weight of 65 kDa. Mucolipin-1 is a membrane protein containing six putative transmembrane domains and both N- and C-termini facing the cytosol. Homology studies reveal that mucolipin-1 is related to transient receptor potential channels, a heterogeneous family of proteins known for their ability to conduct monovalent and divalent cations (15). This homology has led to the suggestion that mucolipin-1 functions as an ion channel. In agreement with this idea, the expression of the protein in oocytes or artificial liposomes demonstrated that mucolipin-1 behaves as a non-selective cation channel permeable to Ca^{2+}, Na^{+} and K^{+} and that its activity is modulated by changes in pH and Ca^{2+} concentration (16,17).

Recently, it has been proposed that mucolipin-1 may be involved in the regulation of lysosome biogenesis, and specifically, the reformation of lysosomes from endosome–lysosome hybrid organelles (18). Consistent with this idea, loss-of-function mutations in cup-5, the *Caenorhabditis elegans* ortholog of mucolipin-1, resulted in enlarged vacuoles that resemble endosome–lysosome hybrid organelles based on the presence of both late endosomal and lysosomal markers (19–21).

To elucidate the mechanisms underlying the pathology of MLIV, we analyzed the intracellular trafficking of mucolipin-1. To date, little is known about the targeting information that regulates the transport of this protein to lysosomes or the motifs that mediate interaction with the intracellular sorting machinery. To address these questions, we have generated cDNA constructs encoding chimeric proteins with isolated cytosolic domains of mucolipin-1 attached to a reporter molecule (Tac) or encoding full-length mucolipin-1 with mutations in putative targeting motifs. This strategy has allowed us to identify two independent di-leucine motifs that regulate the delivery of mucolipin-1 to lysosomes. One di-leucine motif is located at the N-terminal tail, and it appears to promote

the transport of mucolipin-1 from the trans-Golgi network (TGN) to early endosomes and subsequently to lysosomes. In contrast, the other di-leucine motif is present at the end of the C-terminal tail and functions as an adaptor protein 2 (AP2)-dependent internalization motif. We have also found that the C-terminal tail of mucolipin-1 is palmitoylated and that this modification may regulate the efficiency of endocytosis.

Results

The C-terminal cytoplasmic tail of mucolipin-1 is sufficient for targeting to early endosomes

To assess whether targeting information is present in the C-terminal cytoplasmic tail of mucolipin-1, a chimeric protein was created in which the last 63 residues of mucolipin-1 were appended to the lumenal and transmembrane domains of Tac, a cell-surface type 1 transmembrane glycoprotein that has been used previously in chimeric constructs to analyze carboxyl-terminal cytoplasmic targeting signals (22). The localization of the chimeric protein, termed Tac-MLN-CTail (for Tac lumenal-Tac transmembrane-Mucolipin-1 C-terminal cytoplasmic tail), was compared with that of intact Tac by indirect immunofluorescence microscopy in HeLa cells using antibodies directed to the Tac lumenal domain. Figure 1A shows that although Tac was distributed mostly at the cell surface with very little in internal structures, Tac-MLN-CTail was present mostly in vesicles scattered through the cytoplasm.

To further characterize the compartment to which the C-terminal tail of mucolipin-1 targeted the Tac antigen, we performed double staining by indirect immunofluorescence analysis to co-localize Tac-MLN-CTail with various endogenous and transfected molecules. As seen in Figure 1B, the Tac-MLN-CTail chimera showed a clear co-localization with early endosomal markers, such as internalized transferrin, Hrs, Rab5-green fluorescent protein (Rab5-GFP) or its constitutively active version, Rab5-Q79L-GFP. Conversely, no co-localization was observed with late endosomal or lysosomal markers (*Supplementary Material*, Figure S1). It is interesting to note that the over-expression of Tac-MLN-CTail resulted in swollen endosomes. However, this enlargement did not seem to affect the trafficking of EGF or transferrin (our unpublished results).

Identification of a targeting motif in the C-terminal cytosolic tail of mucolipin-1

It has been previously described that most lysosomal proteins have short cytosolic tails containing tyrosine or di-leucine-based motifs that determine their lysosomal targeting (23). The analysis of the C-terminal cytoplasmic tail of mucolipin-1 revealed the presence of several putative sorting motifs. These include a YXXϕ motif (Y^{521}DTI), a di-leucine motif (L^{563}L) and an acidic di-leucine motif (D/E)XXXL(L/I) (E^{573}EHSLL) (Figure 2A). To determine whether these or other signals were responsible for targeting Tac-MLN-CTail to endosomes, we mutated the three motifs individually by substitution of key residues to alanines, and the resulting immunofluorescence profiles were analyzed in transiently transfected HeLa cells. Figure 2B shows that the mutation of Leu577 and Leu578 to alanines (Tac-MLN-CTail-L^{577}L/AA) caused the protein to be retained at the plasma membrane, whereas the substitution of Tyr521 (Tac-MLN-CTail-Y^{521}/A) or Leu563 (Tac-MLN-CTail-L^{563}/A) with alanines had no effect on the distribution of the chimeras.

To determine whether the (D/E)XXXL(L/I) motif acts as a signal for internalization from the cell surface, we performed antibody-uptake experiments. Antibodies to Tac were bound on ice to the surface of HeLa cells expressing Tac, Tac-MLN-CTail or Tac-MLN-CTail-L^{577}L/AA, then bound antibody was allowed to internalize for 15 min at 37 °C, and the amount of protein remaining at the cell surface was quantified by flow cytometry (FACS). As seen in Figure 2C, nearly 60% of the antibody initially bound to Tac-MLN-CTail was internalized by 15 min. In contrast, no internalization was observed for the Tac-MLN-CTail-L^{577}L/AA chimera. These data indicate that the E^{573}EHSLL sequence is an essential component of the endosomal targeting signal in mucolipin-1 cytoplasmic tail.

Endocytosis of Tac-MLN-CTail is dependent on clathrin adaptor AP2

It has been extensively studied that (D/E)XXXL(L/I) motifs are recognized with high specificity by the AP complexes. Four different AP complexes have been described and termed AP1, AP2, AP3 and AP4. Although all four complexes participate in cargo selection and vesicle formation in the endocytic and secretory pathways, they exhibit distinct intracellular localizations. AP2 is exclusively located at the plasma membrane and plays an essential role in the endocytosis of specific cargo proteins. To address whether AP2 participates in the internalization of the Tac-MLN-CTail chimera, we reduced the expression of endogenous AP2 in HeLa cells using specific siRNA oligonucleotides. Immunoblot analysis revealed a 90% reduction in the levels of AP2 when compared with cells transfected with control (non-silencing) siRNA (Figure 3A). The levels of annexin-II were monitored as control for the specificity of the antisense. As expected, HeLa cells depleted of AP2 showed very little internalization of rhodamine-transferrin when compared with control cells, indicating that AP2-dependent endocytosis is impaired (Figure 3B). Likewise, FACS analysis revealed that the internalization of Tac-MLN-CTail was blocked in the absence of AP2. Figure 3C shows that in cells treated with control non-silencing siRNA approximately 35% of Tac-MLN-CTail remained at the plasma membrane after 15 min internalization. In contrast, almost no endocytosis of Tac-MLN-CTail was observed in cells depleted of AP2. In addition, surface staining of

Tac-MLN-CTail showed a good co-localization between the chimera and AP2-GFP in structures that resemble clathrin-coated-pits (Figure 3D). Altogether, these results indicate that the E^{573}EHSLL sequence can mediate the internalization of Tac-MLN-CTail through an AP2-dependent pathway.

Palmitoylation mediates the association of the C-terminal tail of mucolipin-1 with membranes

We found that the C-terminal cytosolic tail of mucolipin-1 is sufficient to promote the recruitment of GFP to intracellular membranes. As seen in *Supplementary Material*, Figure and Figure 4A, the expression of a chimera containing the

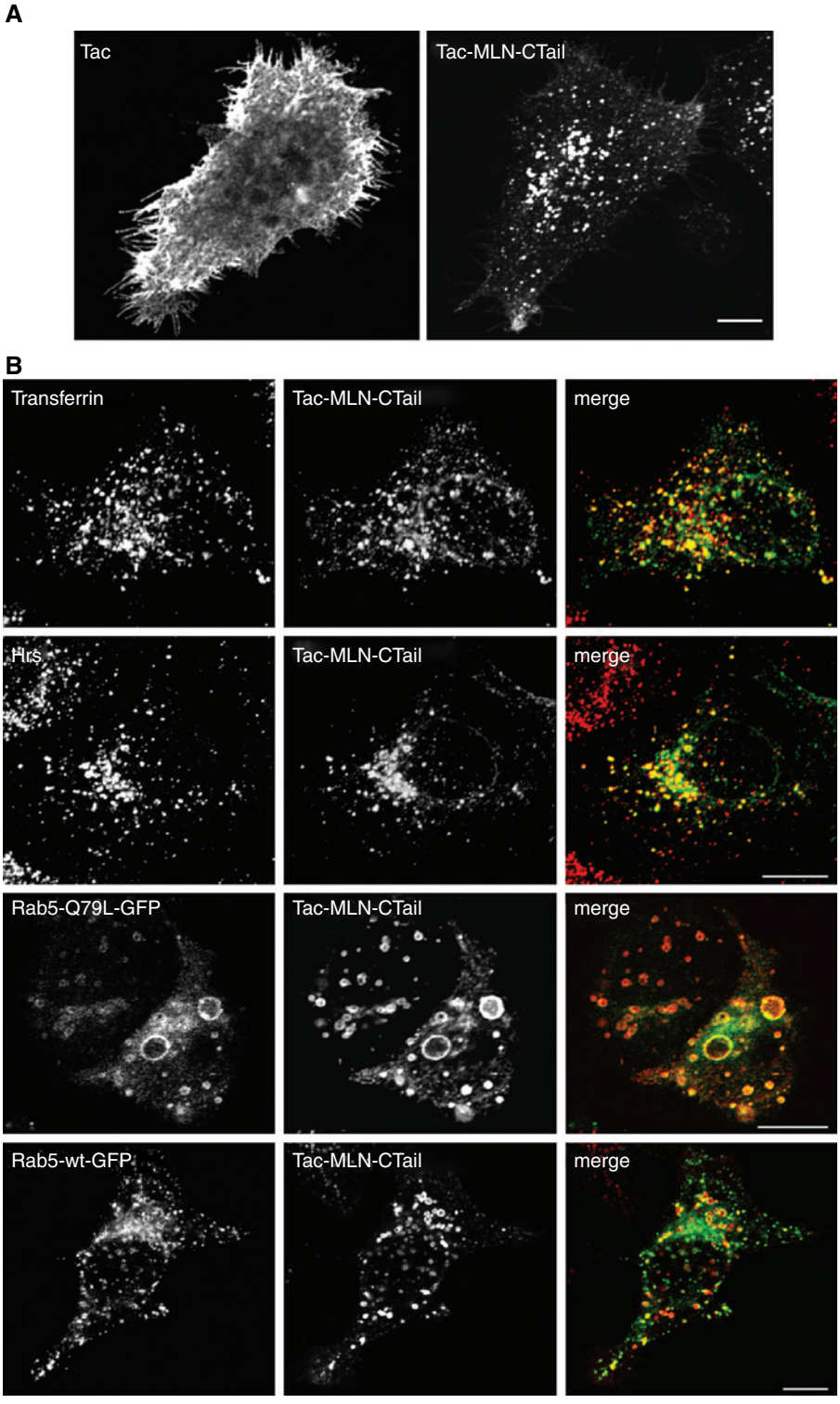

Figure 1: The C-terminal tail of mucolipin-1 contains sorting information for location to early endosomes. (A) HeLa cells were transfected with plasmids encoding Tac alone (left panel) or a chimera made by fusing the C-terminal tail of mucolipin-1 to the extracellular and transmembrane domains of Tac (Tac-MLN-CTail) (right panel). Refer to Figure 2A for the schematic of the chimera. (B) HeLa cells were transfected with plasmids encoding Tac-MLN-CTail alone (first and second row) or in combination with Rab5-Q79L-GFP or Rab5-GFP (third and fourth row, respectively). Transfected cells were fixed, permeabilized and immunostained with a monoclonal antibody to Tac followed by a Cy3-conjugated donkey anti-mouse IgG (for double immunofluorescence with GFP) or an Alexa488-conjugated goat anti-mouse IgG (for double staining with transferrin and Hrs). Cells were examined by confocal fluorescence microscopy. For transferrin staining, cells were incubated with rhodamine-transferrin for 15 min at 37 °C. For Hrs staining, cells were incubated with a polyclonal antibody to Hrs followed by an Alexa555-conjugated goat anti-rabbit IgG. Merging images in the red and green channels generated the third picture on each row; yellow indicates overlapping localization. Scale bar represents 10 μm.

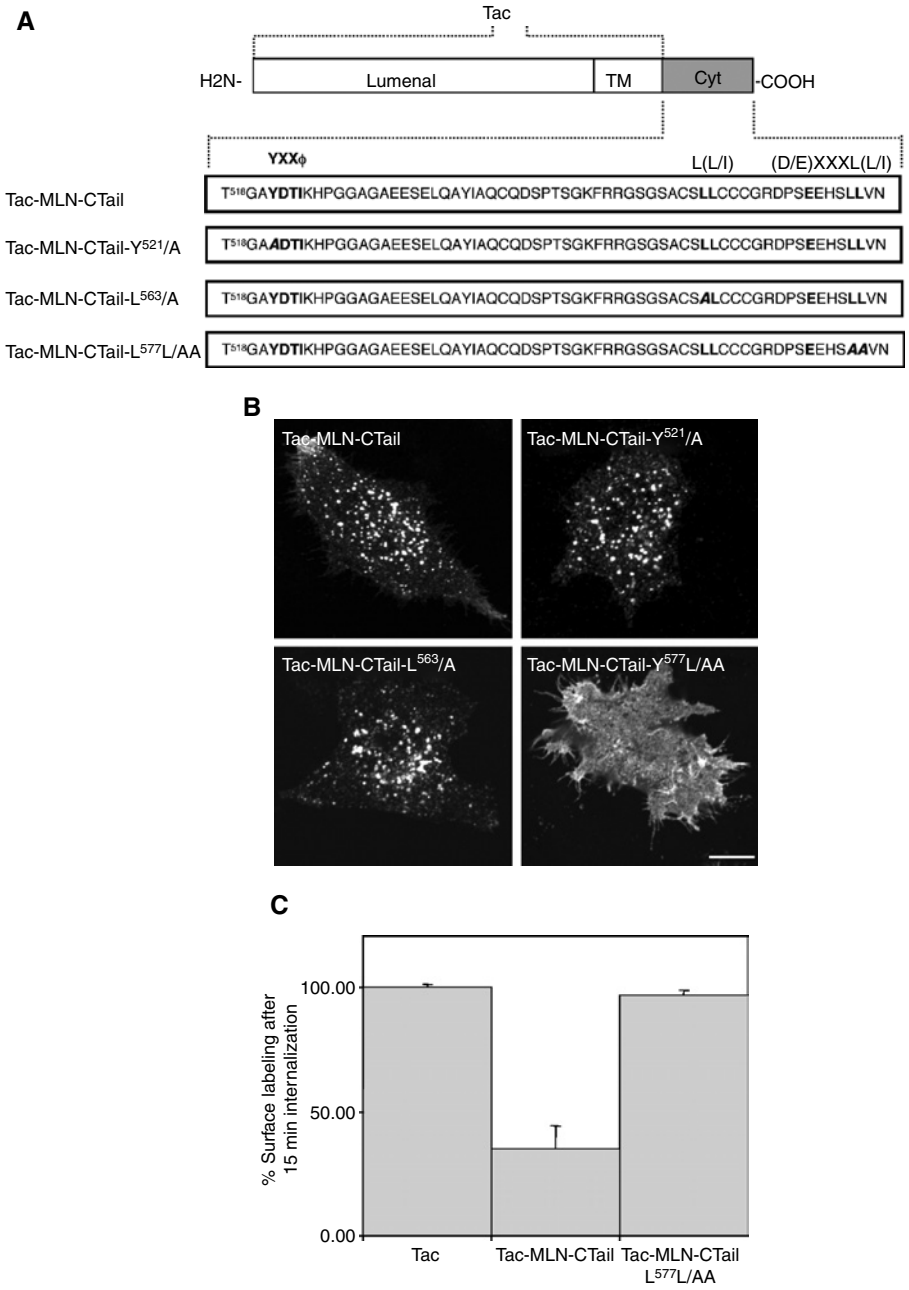

Figure 2: A di-leucine motif located at C-terminal tail of mucolipin-1 mediates internalization of Tac-MLN-CTail chimera. (A) Putative sorting motifs present at the C-terminal tail of mucolipin-1 and sorting motif mutations to alanines. The lumenal and transmembrane (TM) domains of Tac as well as the C-terminal tail of mucolipin-1 (Cyt) are indicated. (B) Wild-type Tac-MLN-CTail or Tac-MLN-CTail carrying the indicated mutations was transiently expressed in HeLa cells, incubated for 1 h on ice with monoclonal antibodies to the extracellular domain of Tac, washed and allowed to internalize for 15 min at 37 °C. Cells were then fixed, permeabilized, stained with a Cy3-conjugated donkey anti-mouse IgG and analyzed by confocal fluorescence microscopy. Bar represents 10 μm. (C) Cell-surface levels of Tac, Tac-MLN-CTail or Tac-MLN-Ctail-L^{577}L/AA were analyzed by FACS, as described in *Materials and Methods*. Results are expressed as the percentage of Tac chimera remaining at the cell surface after 15 min incubation at 37 °C. Values represent the mean ± SD from four independent experiments.

C-terminal tail of mucolipin-1 fused to GFP (GFP-MLN-CTail) showed staining of the plasma membrane and cytosolic vesicles. The vesicles strongly co-localized with early endosomal markers such as internalized transferrin, EEA1 and Hrs, as well as with Tac-MLN-CTail (*Supplementary Material*, Figure S2). These data indicate that the C-terminal tail of mucolipin-1 has the ability to associate with membranes independently of the presence of a transmembrane domain, suggesting that acylation may be responsible for the observed sub-cellular targeting.

Our examination of the sequence of the mucolipin-1 C-terminal tail revealed the presence of four cysteines (**C**^{561}SLL**CCC**) that appear to be likely candidates to undergo palmitoylation via thioester linkages. To assess whether palmitoylation might be responsible for the association of the mucolipin-1 C-terminal tail with intracellular membranes, we incubated HeLa cells expressing GFP-MLN-CTail for 12 h with 2-bromopalmitate (2-BP), a potent inhibitor of protein palmitoylation (24). As predicted, in cells treated with 2-BP, GFP-MLN-CTail exhibited no detectable membrane staining but instead displayed a diffuse cytoplasmic staining (Figure 4A). Next, we carried out systematic mutagenesis of the C^{561}SLLCCC sequence by individually substituting each of these residues with alanines and analyzing the location of the resulting

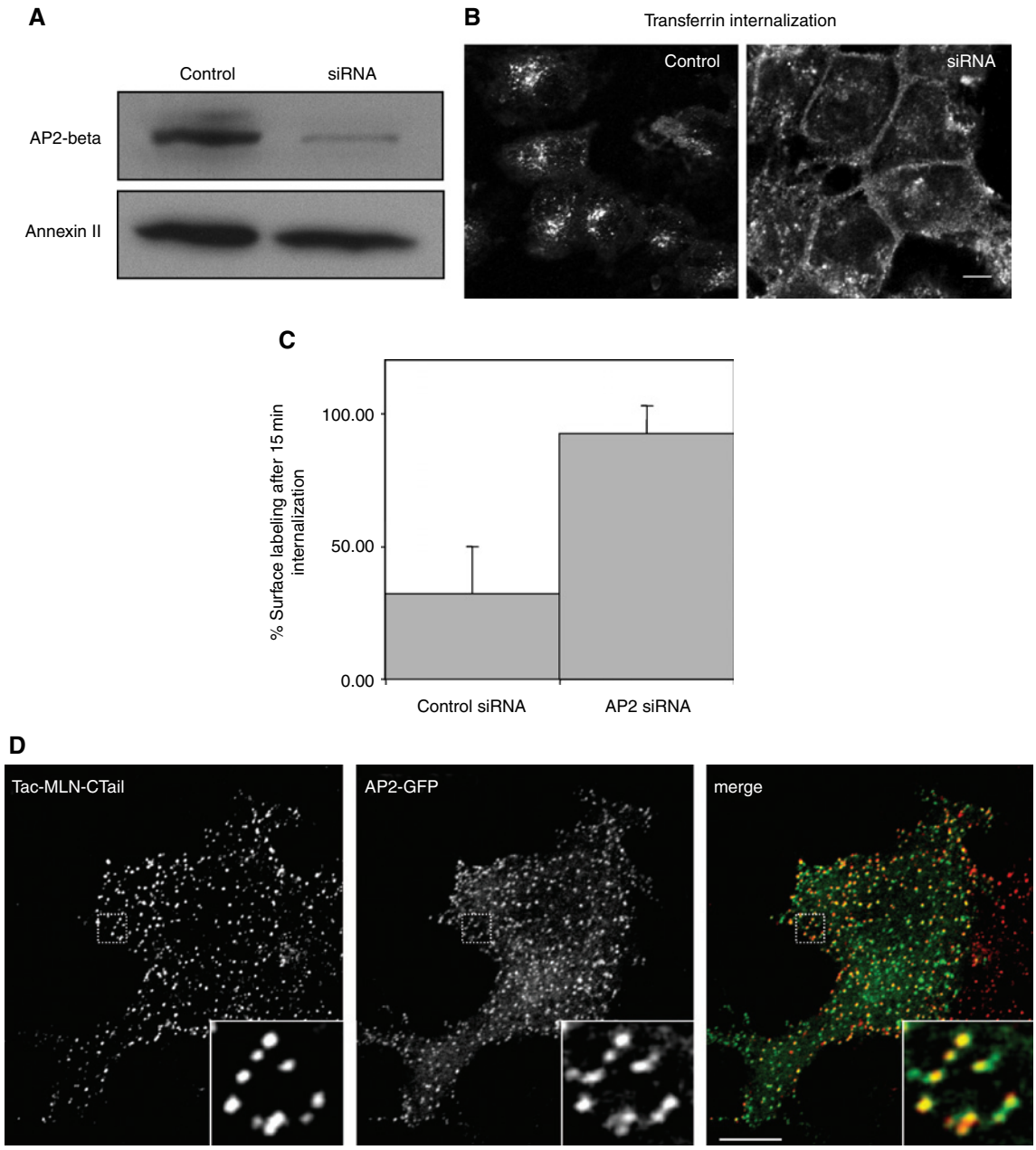

Figure 3: Endocytosis of Tac-MLN-CTail is dependent on clathrin adaptor AP2. (A) HeLa cells were transfected with siRNA targeted to control (non-silencing) or to the μ2 subunit of the AP2 complex. Seventy-two hours after the second round of transfection, equivalent amounts of homogenate from control and siRNA-treated cells were subjected to SDS-PAGE and immunoblotted using antibodies to the β2 subunit of AP2 or annexin-II (loading control). (B) Control and siRNA-treated HeLa cells were incubated with rhodamine-transferrin for 15 min at 37 °C and analyzed by confocal microscopy. (C) HeLa cells treated with non-targeted siRNA or siRNA against AP2 were transfected with Tac-MLN-Ctail, and the amount of the chimera present at the plasma membrane was quantified by FACS analysis. Results are expressed as the percent of Tac-MLN-CTail remaining at the cell surface after 15 min incubation at 37 °C. Values represent the mean ± SD from two independent experiments. (D) HeLa cells were co-transfected with Tac-MLN-CTail and AP2-GFP, incubated for 1 h on ice with monoclonal antibody to the extracellular domain of Tac, washed and allowed to internalize for 1 min at 37 °C. Cells were then fixed, permeabilized, stained with a Cy3-conjugated donkey anti-mouse IgG and analyzed by confocal fluorescence microscopy. Insets show a fourfold magnification of the indicated region. Bars represent 10 μm.

chimeras by confocal microscopy. The results are summarized in Table 1 Interestingly, the substitution of the three cysteine residues located between positions 565 and 567 with alanines (GFP-MLN-CTail-C^{565}CC/AAA) abolished the ability of the C-terminal tail of mucolipin-1 to associate with membranes (Table 1; Figure 4A). Individual mutation of each of these three cysteines revealed that Cys566 is essential for recruitment to

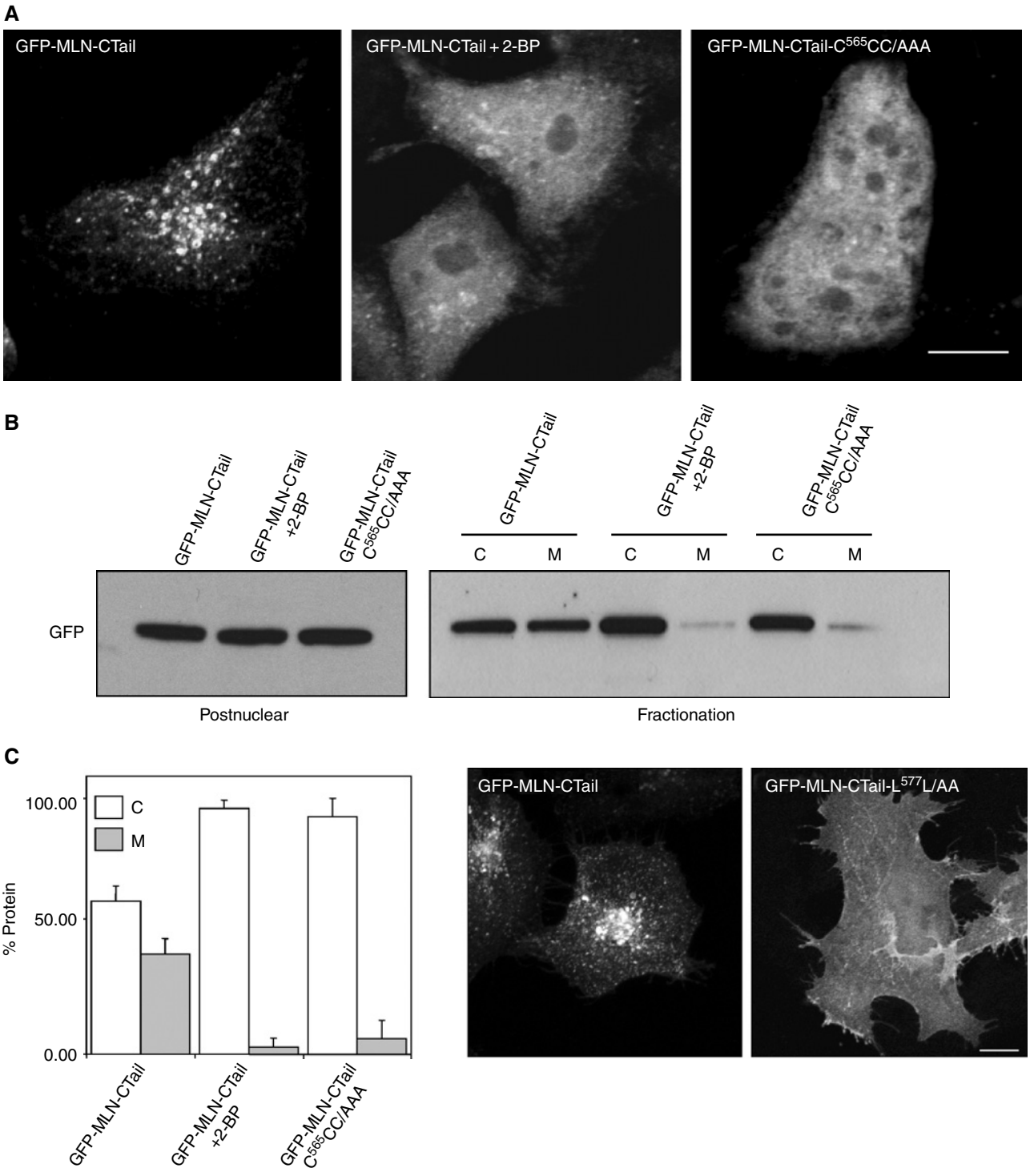

Figure 4: Palmitoylation of three cysteine residues mediates recruitment of GFP-MLN-CTail to membranes. (A) HeLa cells were transfected with either GFP-MLN-CTail, in the presence of ethanol or the inhibitor of palmitoylation 2-bromopalmitate (2-BP), or GFP-MLN-CTail-C^{565}CC/AAA and analyzed by confocal microscopy. (B) Transfected HeLa cells were fractionated into cytosol (C) and membrane fractions (M). The distribution of GFP-MLN-CTail in the presence or absence of 2-BP, and GFP-MLN-Tail-C^{565}CC/AAA was determined by immunoblotting using a GFP-specific antibody. Equivalent volumes of cytosol and membrane fractions were loaded. (C) Quantification of the optical densities of the corresponding GFP bands averaged from (B) from two independent experiments. (D) HeLa cells were transfected with either GFP-MLN-CTail or GFP-MLN-CTail-L^{577}L/AA and analyzed by confocal microscopy. Bars represent 10 μm.

Table 1: Mutational analysis of the C-terminal tail of mucolipin-1

Sequence	Membrane association	Localization
A^{560}**CSLLCCC**GRDPSEEHS**LL**VN	+++	Endosomes/plasma membrane
A^{560}***A*SLLCCC**GRDPSEEHSLLVN	+++	Endosomes/plasma membrane
A^{560}**C*A*LLCCC**GRDPSEEHSLLVN	+++	Endosomes/plasma membrane
A^{560}**CS*AA*CCC**GRDPSEEHSLLVN	–	Cytosol
A^{560}**CS*A*LCCC**GRDPSEEHSLLVN	+++	Endosomes/plasma membrane
A^{560}**CSL*A*CCC**GRDPSEEHSLLVN	–	Cytosol
A^{560}**CSLL*AAA***GRDPSEEHSLLVN	–	Cytosol
A^{560}**CSLL*A*CC**GRDPSEEHSLLVN	–/+	Cytosol/endosomes/plasma membrane
A^{560}**CSLLC*A*C**GRDPSEEHSLLVN	–	Cytosol
A^{560}**CSLLCC*A***GRDPSEEHSLLVN	–/+	Cytosol/endosomes/plasma membrane
A^{560}**CSLLCCC**	+++	Plasma membrane
A^{560}**CSLLCCC**GRDPSEEHS***AA***VN	+++	Plasma membrane

Wild-type GFP-MLN-CTail or GFP-MLN-CTail carrying the indicated mutations (in red) was expressed in HeLa cells, and their association with membranes was assayed by immunofluorescence microscopy.

membranes, whereas the mutation of Cys565 or Cys567 had only a partial effect on the ability of the chimeras to interact with intracellular membranes. The mutation of Leu564 to alanine also caused redistribution to the cytosol, suggesting that this amino acid is required for optimal palmitoylation. In contrast, the substitution of Cys561, Ser562 or Leu563 with alanine did not affect the distribution of the chimeras. Interestingly, a mutant that lacks the last 13 residues but still contains Cys565, Cys566 and Cys567 retained its ability to associate with membranes but was localized exclusively to the plasma membrane. Similarly, the substitution of Leu577 and Leu578 with alanine also resulted in the redistribution of chimera to the plasma membrane (Figure 4D). These data suggest that the C^{565}CC sequence is required for palmitoylation and subsequent association with membranes although the acidic di-leucine motif mediates localization at endosomes.

To further confirm the role of palmitoylation on the membrane partitioning of the GFP chimeras, we fractionated cellular lysates from cells expressing the above chimeras into cytosolic (C) and membrane (M) fractions through high-speed ultracentrifugation. Figure 4B,C shows that approximately 50% of GFP-MLN-CTail partitioned into the membrane-associated fractions, whereas GFP-MLN-CTail-C^{565}CC/AAA was predominantly soluble. The treatment of cells expressing GFP-MLN-CTail with 2-BP also caused the redistribution of chimera to the soluble fraction. In comparison, non-palmitoylated Rab5 localization was not altered by 2-BP treatment, indicating that the drug is specific in blocking modification by palmitate (data not shown). These results corroborate that preventing palmitoylation by cysteine-to-alanine mutations or 2-BP treatment blocks the ability of the C-terminal tail of mucolipin-1 to stably bind to membranes.

Palmitoylation regulates the efficiency of internalization of Tac-MLN-CTail

It has been described that the position of sorting motifs relative to the transmembrane domain may influence the affinity of the interaction with the sorting machinery (23). In the case of endocytic signals, they are often (although not always) situated at proximity from the membrane. This proximity could facilitate the interaction of AP2 with specific lipids such as phosphatidylinositol 4,5-biphosphate (PIP2) or other PIP2-binding proteins. Interestingly, the proximity of a sorting motif to the membrane may be shortened by palmitoylation. It has been reported that the palmitoylation of specific cysteine residues in the cytosolic tail of the cation-dependent mannose 6-phosphate receptor may serve to anchor this domain closer to the membrane by insertion of the palmitoyl chains into the lipid bilayer (25).

Consistent with this idea, we hypothesized that palmitoylation of the C^{565}CC site could help bring the E^{573}EHSLL signal closer to the plasma membrane, thus facilitating endocytosis. To address this possibility, we compared the efficiency of internalization of Tac, Tac-MLN-CTail and Tac-MLN-CTail-C^{565}CC/AAA by FACS. As shown in Figure 5, the percent of Tac-MLN-CTail-C^{565}CC/AAA that is internalized after 15 min was reduced to almost half when compared with that of Tac-MLN-Ctail (35% versus 61%). Together, our results suggest that the palmitoylation of the C-terminal tail of mucolipin-1 may play a role in regulating its trafficking possibly through bringing the endocytic signal closer to the plasma membrane, thus increasing the efficiency of endocytosis.

To test whether full-length mucolipin-1 was palmitoylated, we transfected mucolipin-1 wild-type (MLN-GFP; see below) as well as a mutant lacking the putative palmitoylated cysteines (MLN-GFP-C^{565}CC/AAA) into HeLa cells and metabolically labeled these cells with [^{3}H]palmitate followed by immunoprecipitation and SDS-PAGE. As seen in Figure 5B, the immunoprecipitation of full-length mucolipin-1 revealed a band of approximately 90 kDa that corresponds to the predicted molecular weight of the chimera and was labeled with [^{3}H]palmitate. In contrast, no metabolic labeling was observed for the MLN-GFP-C^{565}CC/AAA mutant. Therefore, we conclude that mucolipin-1 is palmitoylated *in vivo*

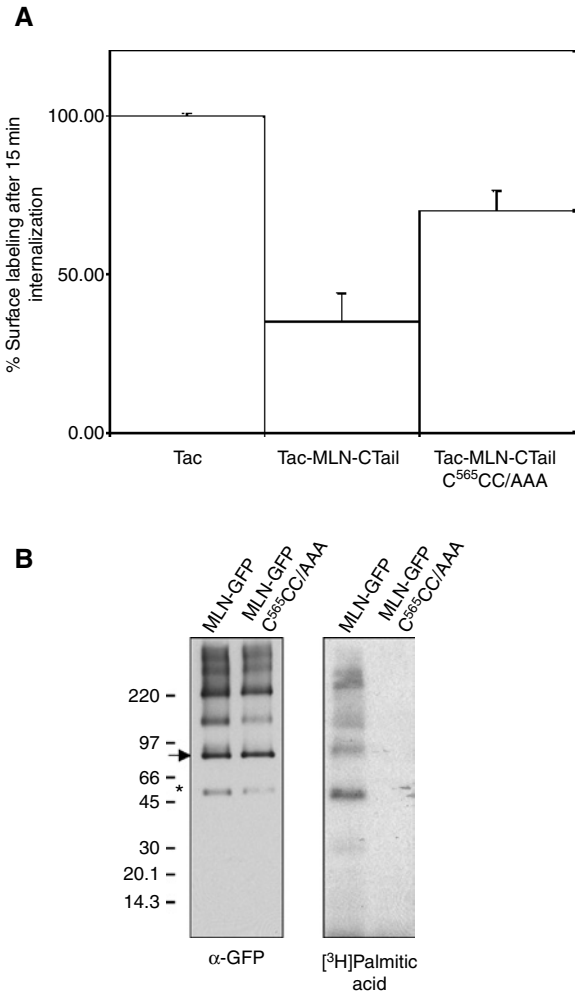

Figure 5: Effect of palmitoylation on the internalization of Tac-MLN-CTail. (A) Internalization of Tac, Tac-MLN-CTail and Tac-MLN-CTail-C^{565}CC/AAA was analyzed by FACS, as described in *Materials and Methods*. Results are expressed as the percentage of Tac chimera remaining at the cell surface after 15 min incubation at 37 °C. The graphic shows the average results from four independent experiments. (B) HeLa cells transfected with MLN-GFP or MLN-GFP-C^{565}CC/AAA were metabolically labeled with [^{3}H]palmitic acid for 6 h. Cells were then lysed, immunoprecipitated with an anti-GFP polyclonal antibody, subjected to SDS-PAGE and analyzed either by Western blotting using an anti-GFP monoclonal antibody (left panel) or by fluorography and autoradiography (right panel). Film was exposed for 15 days at −80 °C. Arrow corresponds to the predicted molecular weight of the monomeric form of the full-length MLN-GFP fusion protein, whereas the asterisk corresponds to a putative proteolytic form. Higher bands probably correspond to dimers and oligomers of MLN-GFP.

and that Cys565, Cys566 and Cys567 account for the total palmitoylation of the protein.

Full-length mucolipin-1 contains additional sorting information that regulates its transport to lysosomes

We next analyzed the distribution of full-length mucolipin-1. To do so, we generated a chimera in which GFP was fused to the C-terminal end of mucolipin-1 (MLN-GFP). When transiently transfected into HeLa cells, MLN-GFP localized in vacuolar structures containing late endosomal–lysosomal markers such as CD63 and lamp-1 (Figure 6). In contrast, no significant co-localization with early endosomal markers was observed (data not shown). This distribution is consistent with recent data showing that cup-5, the *C. elegans* ortholog of mucolipin-1, is present in both mature lysosomes and specific subdomains of late endosomes where endosomal cargo destined for the lysosome accumulates (21). In addition, Manzoni et al. (26) have recently described that a myc-epitope tagged version of mucolipin-1 mostly co-localizes with lamp-1. It has been suggested that mucolipin-1 could play an important role in the regulation of lysosomal biogenesis. In agreement with this idea, we found that the over-expression of MLN-GFP in HeLa cells caused a dramatic enlargement of lysosomes. These structures resemble the late endosome–lysosome hybrid organelles observed in cup-5-defective cells (see arrows in Figure 6). Interestingly, very little co-localization was observed between Tac-MLN-CTail and MLN-GFP, indicating that additional sorting information, located in a region different from the C-terminal tail, mediates the transport of the full-length mucolipin-1 to lysosomes.

The N-terminal cytoplasmic tail of mucolipin-1 contains targeting information for sorting to lysosomes

The search for sorting sequences that mediate the delivery of mucolipin-1 to lysosomes revealed the presence of a (D/E)XXXL(L/I) motif (**E**^{11}TER**LL**) at the N-terminal cytosolic tail of the protein that could potentially mediate interaction with APs and transport to lysosomes. To determine whether this motif is in fact functional, we fused the N-terminal tail of mucolipin-1 (residues from positions 1 to 66) to the extracellular and transmembrane domains of Tac, and the distribution of the resulting chimera (Tac-MLN-NTail) was analyzed by confocal microscopy. As shown in Figure 7A, Tac-MLN-NTail localized predominantly to large vesicular structures within the cytoplasm. To determine the nature of these vesicles, we monitored EGF uptake using EGF-Alexa Fluor 555. EGF binds to its receptor on the cell surface, and receptor–ligand complexes are internalized by clathrin-coated vesicles and transported to lysosomes for degradation. After uptake for 30 min, EGF labeled small vesicles throughout the cytoplasm that correspond to early and/or late endosomes and did not contain Tac-MLN-NTail. In contrast, after 3 h of internalization, EGF accumulated at lysosomes and showed good co-localization with Tac-MLN-NTail. Extensive co-localization was also observed between Tac-MLN-NTail and MLN-GFP. These results indicate that the N-terminal tail of mucolipin-1 contains sorting information for transport to lysosomes.

To be sure that the cloning of the N-terminal tail fused to Tac in a 'type I' orientation (instead of the 'type II' conformation that this fragment has in mucolipin-1) was not

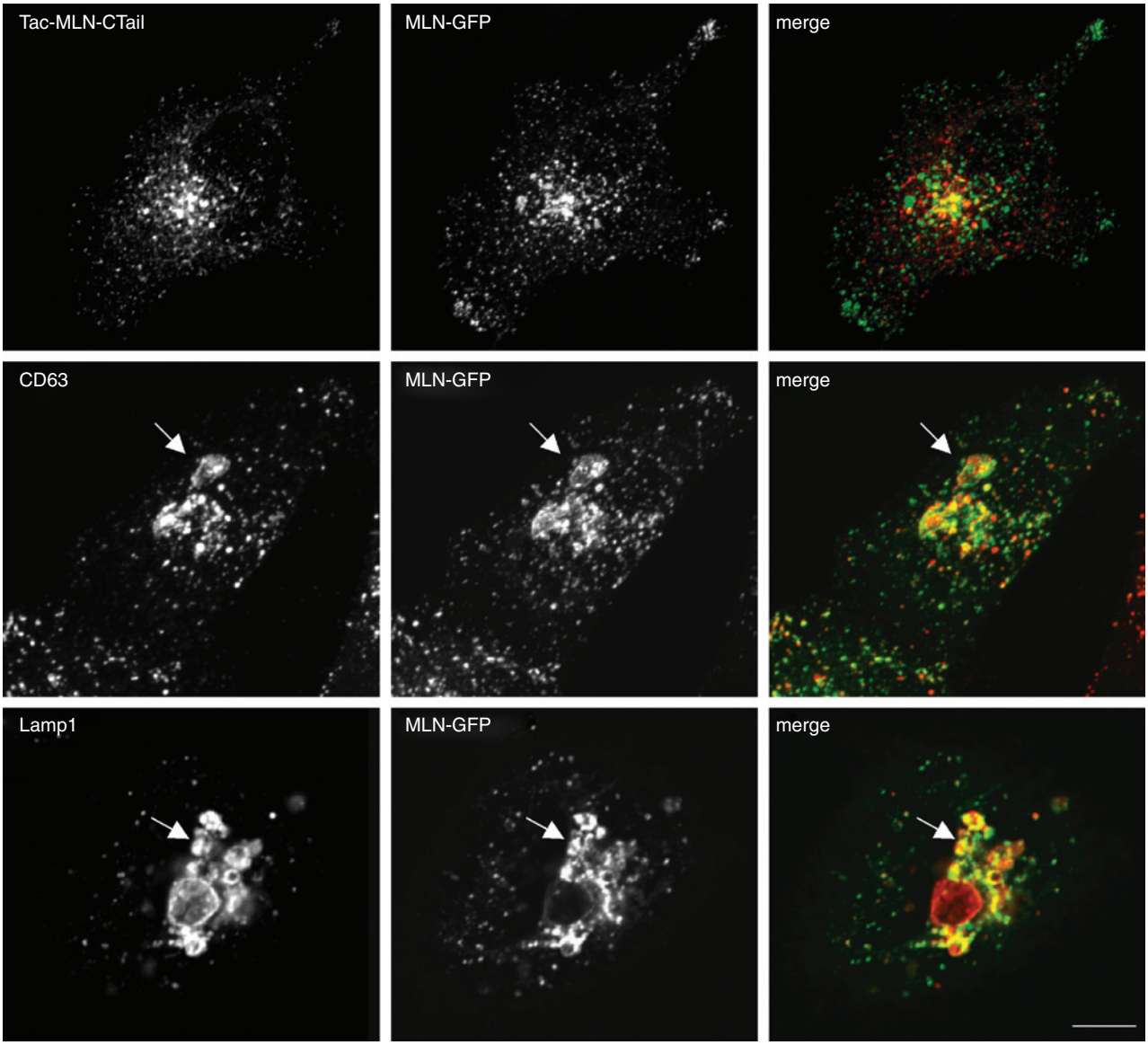

Figure 6: Full-length mucolipin-1 contains additional sorting signals that regulate its transport to lysosomes. HeLa cells were transfected with MLN-GFP alone (second and third row) or in combination with Tac-MLN-CTail (first row). Fifteen hours after transfection, cells were incubated with 100 μg/mL of cycloheximide for 6 h to allow efficient exit from the ER, fixed, permeabilized and immunostained with the indicated antibodies. MLN-GFP is in green; Tac-MLN-Tail, lamp-1 and CD63 are in red; yellow indicates co-localization. Bar represents 10 μm.

affecting the sorting of the chimera, we generated a construct in which the NTail of mucolipin-1 was fused to the transmembrane and extracellular domains of the transferrin receptor (TfR). Our data showed that the MLN-NTail-TfR-GFP chimera is partially delivered to lysosomes (as seen by co-localization with lamp-1), whereas wild-type TfR-GFP localizes at early endosomes and plasma membrane (data not shown). These results corroborate the presence of lysosomal sorting motifs at the N-terminal tail and indicate that the transport of Tac-MLN-NTail to lysosomes is not a consequence of the 'reverse' orientation of the chimera.

One interesting observation from our previous experiment was that Tac-MLN-NTail could only be detected after incubation of the cells with the lysosomal inhibitor leupeptin. This suggests that after the synthesis of the protein, Tac-MLN-NTail is rapidly transported to lysosomes for degradation. To test this hypothesis, we followed the fate of newly synthesized Tac-MLN-NTail by performing 'pulse–chase' experiments by treatment with Brefeldin A (BFA). This approach has been recently used to monitor the transport of LEP100 and CD63 to lysosomes (27). HeLa cells were transfected with the Tac-MLN-NTail or the Tac-MLN-CTail chimera, and 6 h after transfection, the

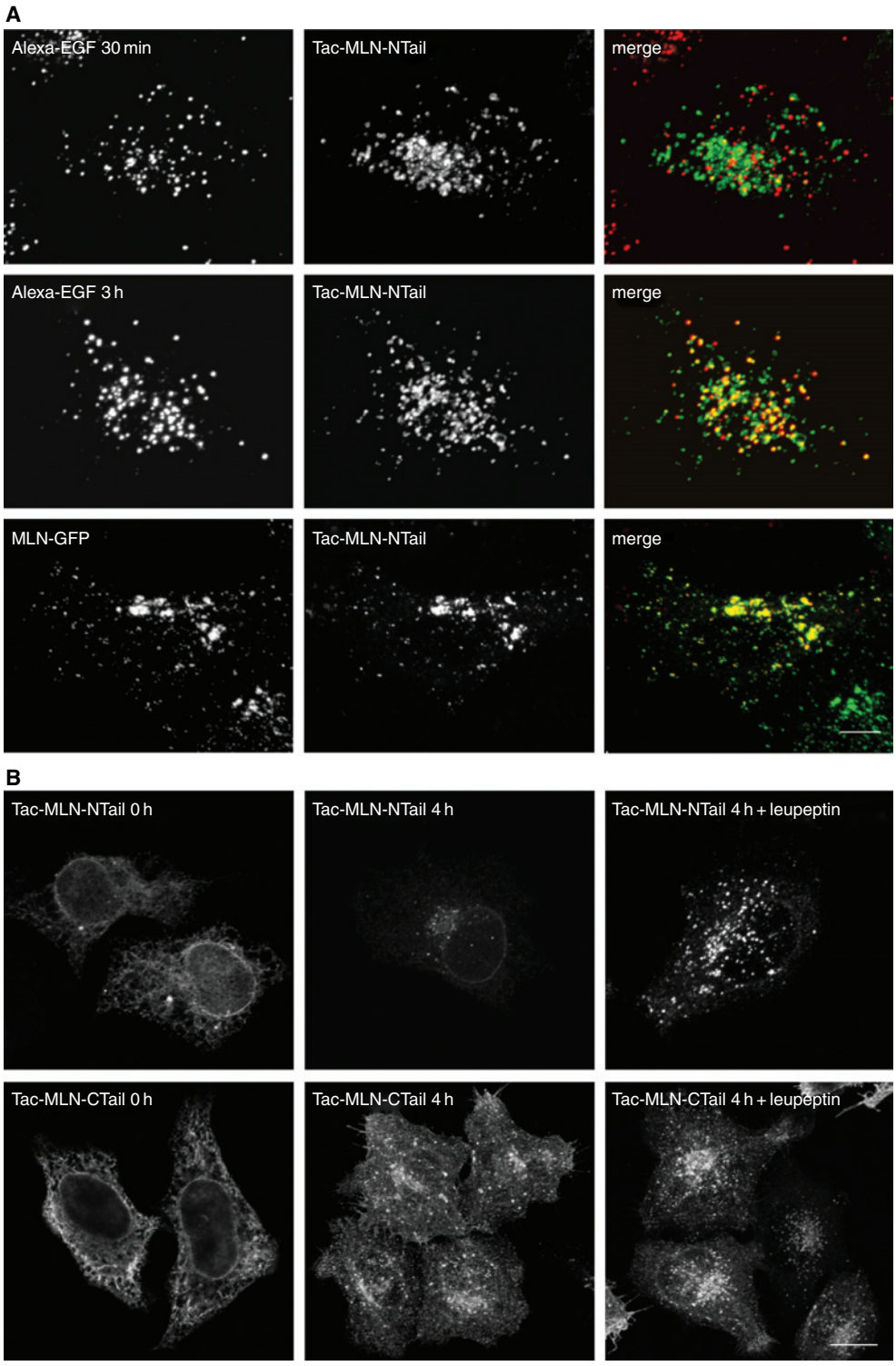

Figure 7: The N-terminal tail of mucolipin-1 contains sorting information for transport to lysosomes. (A) HeLa cells expressing Tac-MLN-NTail (green) were incubated with Alexa555-EGF for 10 min, washed and allowed to internalize for 30 min to load early–late endosomes (first row), or for 3 h to stain lysosomes (second row) in the presence of 20 μM leupeptin. The third row shows HeLa cells co-expressing Tac-MLN-NTail and MLN-GFP treated for 5 h with 100 μg/mL of cycloheximide and 20 μM leupeptin. Refer to Figure 8B for schematics of the chimeras. (B) HeLa cells were transfected with Tac-MLN-NTail (first row) or Tac-MLN-Ctail (second row). Six hours after transfection, the cells were incubated for an additional 12 h in the presence of 2 μg/mL of Brefeldin A (BFA). BFA was then removed, and the cells were incubated for the indicated periods of time at 37 °C in the absence or presence of 20 μM leupeptin. Cells were fixed and permeabilized, and the distribution of the chimeras was revealed by indirect immunofluorescence staining and confocal microscopy. Bars represent 10 μm.

cells were incubated with 2 μg/mL of BFA for 12 h to accumulate the newly synthesized proteins in the endoplasmic reticulum (ER) (28). Proteins were then released from the ER by incubation in medium without BFA, and cells were analyzed at different time-points. We found that, whereas the levels of Tac-MLN-CTail remained stable, most of Tac-MLN-NTail labeling disappeared after a 4-h chase. As expected, the degradation of Tac-MLN-NTail was inhibited in the presence of leupeptin, indicating that the degradation of the protein occurs at lysosomes (Figure 7B).

It is important to note that during the BFA 'pulse–chase' experiments we observed that most of Tac-MLN-CTail reaches the plasma membrane before its location at early endosomes. In contrast, we did not detect Tac-MLN-NTail at the plasma membrane at any time, suggesting that the chimera travels directly from the TGN to the endosomal–lysosomal system. In agreement with this idea, the distribution of Tac-MLN-NTail did not change in cells treated with siRNA against AP2, thus suggesting that the chimera does not travel via the plasma membrane en route to lysosomes. In contrast, most of Tac-MLN-CTail accumulated at the plasma membrane in the absence of AP2 (*Supplementary Material*, Figure).

To determine whether Tac-MLN-NTail passes through early endosomes, we co-expressed the Tac-MLN-NTail chimera together with the constitutively active form of Rab5 (Rab5-Q79L-GFP). It is known that the over-expression of Rab5-Q79L results in enlarged endosomes and interferes with both receptor-mediated and fluid-phase endocytosis (29,30). As seen in Figure 8A, the over-expression of Rab5-Q79L caused the retention of Tac-MLN NTail in early endosomes allowing the detection of the chimera for long periods of time in the absence of leupeptin.

Finally, we addressed whether the (D/E)XXXL(L/I) motif located at the N-terminal tail is responsible for the targeting of Tac-MLN-NTail to lysosomes. As seen in Figure 8B, the mutation of Leu15 and Leu16 to alanines (Tac-MLN-NTail-L^{15}L/AA) abolished the delivery of the resulting chimera to lysosomes, instead causing it to accumulate predominantly at the plasma membrane. These results indicate that the E^{11}TERLL sequence acts as a lysosomal targeting motif regulating the transport of the Tac-MLN-NTail protein from the TGN to lysosomes via early endosomes.

Two di-leucine motifs regulate the transport of mucolipin-1 to lysosomes

The data described above allowed us to conclude the existence of two different sorting motifs, an internalization motif and a lysosomal targeting motif located at the C- and N-terminal tails, respectively. To determine whether these sequences are functional in the context of the full-length protein or whether one of the motifs is preferred, we mutated each of the di-leucine pairs and analyzed the distribution of the resulting proteins by confocal microscopy. Figure 9A shows that the mutation of neither Leu15Leu16 (MLN-GFP-L^{15}L/AA) nor Leu577Leu578 (MLN-GFP-L^{577}L/AA) pair to alanines prevented MNL-GFP from reaching lysosomes (as seen by co-localization with lamp-1, *Supplementary Material*, Figure S4). However, simultaneous mutation of both di-leucine pairs (MLN-GFP-L^{15}L/AA-L^{577}L/AA) resulted in the accumulation of MLN-GFP at the plasma membrane.

Interestingly, the over-expression of Rab5-Q79L-GFP caused a very clear accumulation of MLN-RFP, as well as MLN-RFP-L^{15}L/AA and MLN-RFP-L^{577}L/AA, into Rab5-Q79L-GFP-positive structures indicating that, independently of the route used, mucolipin-1 travels through early endosomes on its way to lysosomes (Figure 9B).

Finally, we addressed whether palmitoylation plays a role in the sorting of full-length mucolipin-1. Data showed that the mutation of the palmitoylation signal alone (MLN-GFP-C^{565}CC/AAA) did not have a clear effect on the trafficking of the protein, as the distribution of MLN-GFP-C^{565}CC/AAA resembled that of MLN-GFP. However, the mutation of Cys565, Cys566 and Cys567 in the MLN-GFP-L^{15}L/AA mutant (MLN-GFP-L^{15}L/AA-C^{565}CC/AAA) or the treatment of MLN-GFP-L^{15}L/AA with 2-BP caused a clear accumulation of the chimeras at the plasma membrane (*Supplementary Material*, Figure).

In conclusion, our results indicate that either one of the di-leucine motifs can mediate the sorting of mucolipin-1 to lysosomes and reveal a role for palmitoylation in the regulation of the protein trafficking.

Discussion

In this study, we have identified two targeting motifs that mediate the trafficking of mucolipin-1 to lysosomes (Figure 10). Both sorting signals are conventional acidic di-leucine motifs ((D/E)XXXL(L/I)) and are located in separate protein domains. One di-leucine motif (E^{11}TERLL) is situated in the N-terminal cytosolic tail and mediates transport to lysosomes when attached to the reporter protein Tac. The other di-leucine motif (E^{573}EHSLL) is positioned at the end of the C-terminal tail and functions as an internalization motif. Interestingly, the mutation of either di-leucine motif alone is not sufficient to prevent the delivery of full-length MLN-GFP to lysosomes. However, simultaneous mutation of both motifs caused the accumulation of MLN-GFP at the plasma membrane.

It has been reported that the trafficking of newly synthesized lysosomal membrane proteins from the TGN to lysosomes may occur through a direct (from TGN to either early or late endosomes, and then to lysosomes) or an indirect pathway (from TGN to plasma membrane

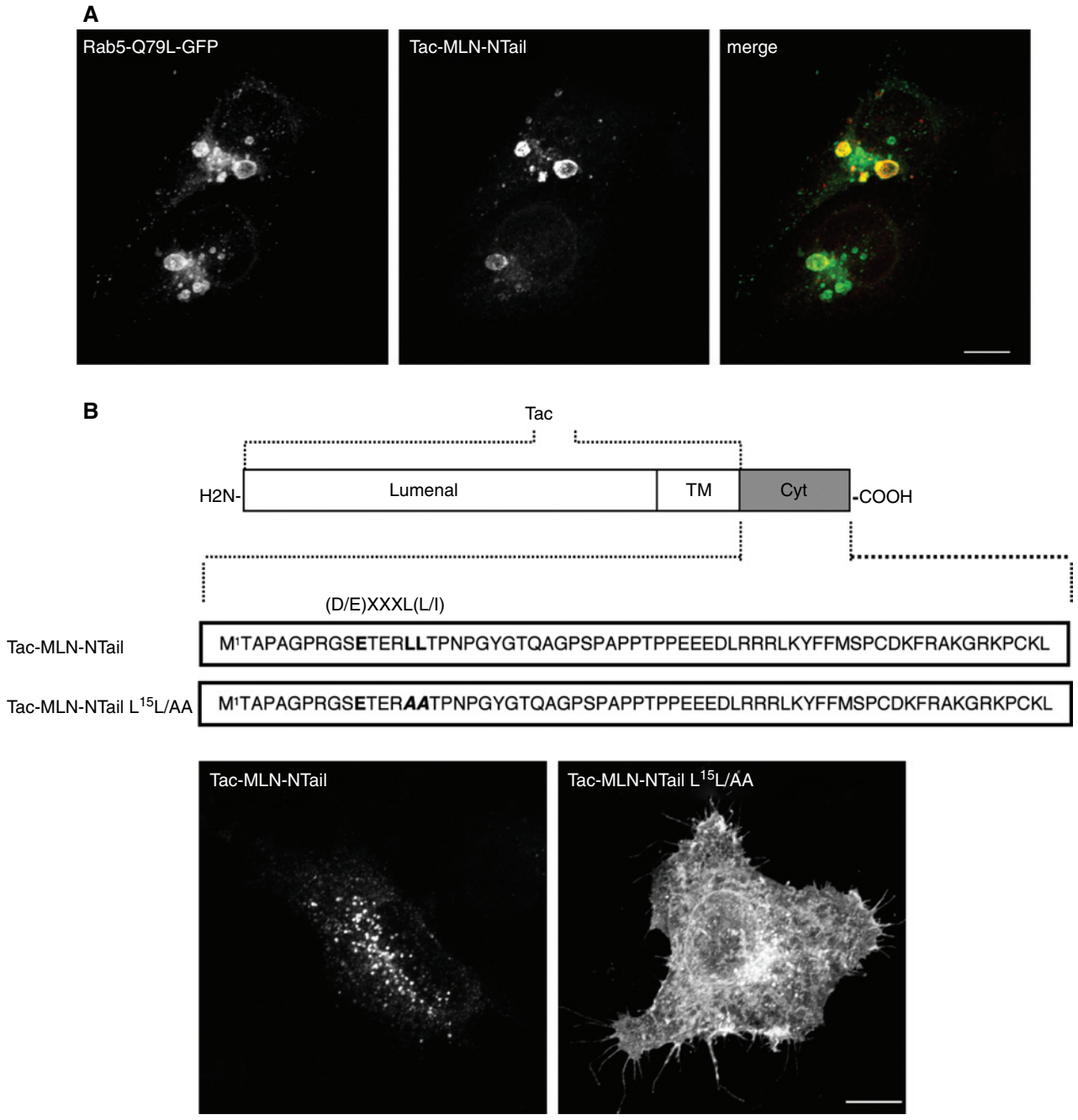

Figure 8: Mutation of a di-leucine motif located at N-terminal tail of mucolipin-1 causes mistargeting of a Tac-MLN-NTail chimera to the plasma membrane. (A) HeLa cells were transfected with Tac-MLN-NTail (red) in combination with Rab5-Q79L-GFP. Leupeptin (20 μM) was added 4 h before fixation of the cells, and the distribution of the chimeras was revealed by indirect immunofluorescence staining and confocal microscopy. (B) HeLa cells expressing wild-type Tac-MLN-NTail or Tac-MLN-NTail carrying alanine mutations at the di-leucine motif (Tac-MLN-NTail-L^{15}L/AA) was analyzed by indirect immunofluorescence staining and confocal microscopy. Sequence of the wild-type and mutated NTail of mucolipin-1 and position of the di-leucine motif are shown above the panels. Bars represent 10 μm.

followed by internalization and sequential delivery to early endosomes, late endosomes and lysosomes). In the case of mucolipin-1, one might predict that the mutation of its lysosomal targeting sequence would cause the default delivery of mucolipin-1 to the plasma membrane from where it would be internalized and delivered to endosomes due to the internalization motif located at the C-terminal tail. In agreement with this idea, MLN-GFP-L^{15}L/AA was able to reach lysosomes but showed clear plasma membrane staining when compared with MLN-GFP. This accumulation at

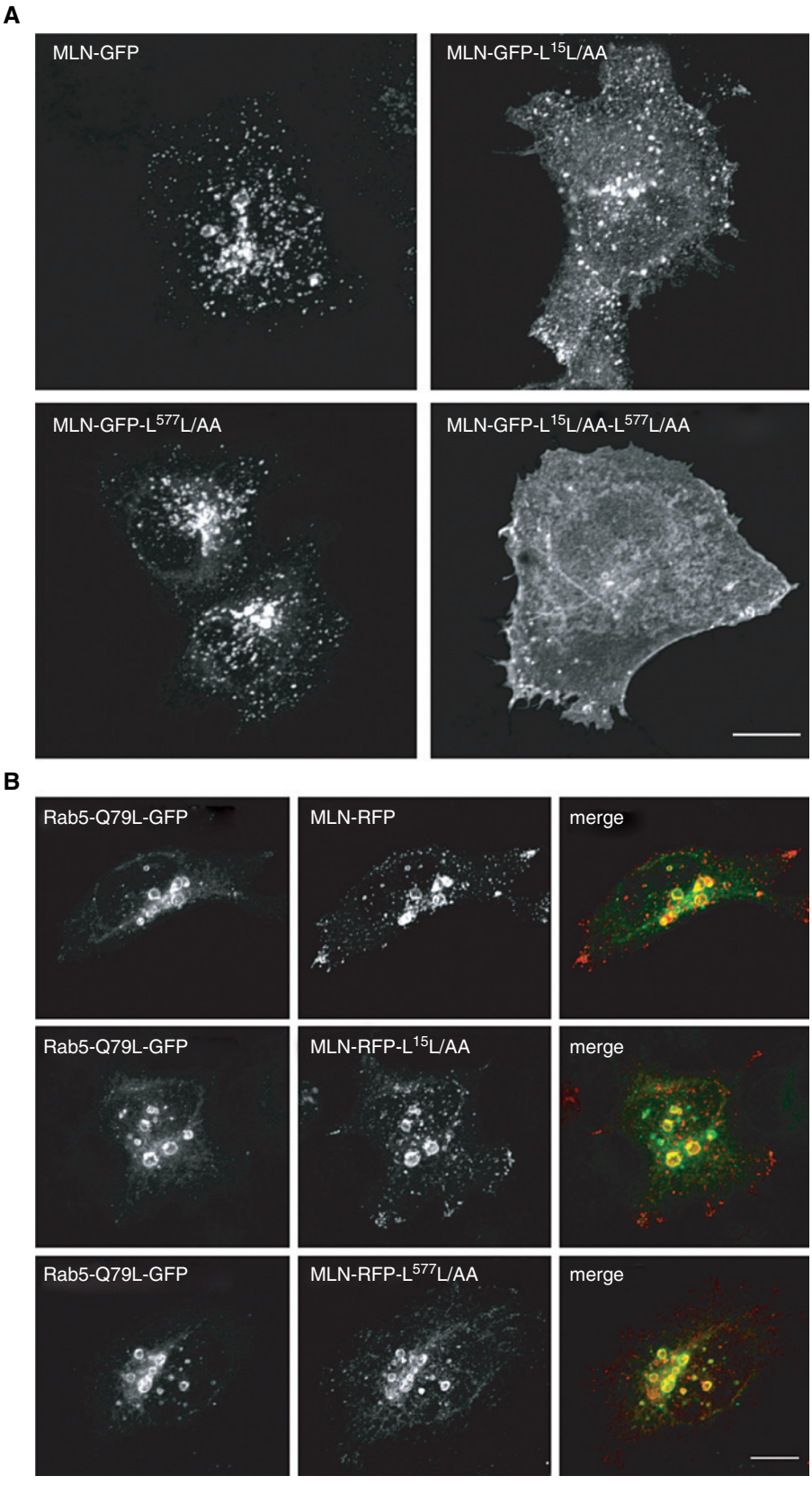

Figure 9: Both di-leucine motifs are required for targeting of mucolipin-1 to lysosomes. (A) Wild-type MLN-GFP or MLN-GFP carrying the indicated mutations was transiently expressed in HeLa cells. Cycloheximide was added for the last 6 h of transfection; cells were then fixed and analyzed by confocal microscopy. (B) Wild-type mucolipin, or the indicated mucolipin mutants, was fused to red fluorescent protein DsRed-Monomer (RFP) and coexpressed with Rab5-Q79L-GFP. Fifteen hours after transfection, cells were treated with cycloheximide for 6 h and analyzed by confocal microscopy. Bars represent 10 μm.

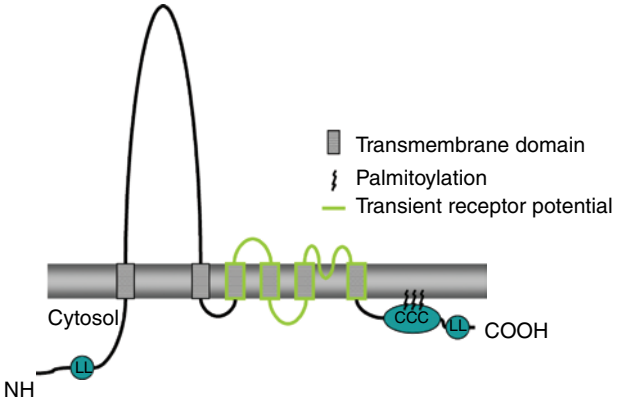

Figure 10: Schematic illustration of the proposed topology of mucolipin-1. Mucolipin-1 has six predicted transmembrane domains, with the N- and C-terminal tails residing in the cytoplasm. The transient receptor potential channel domain is in green. The sorting motifs identified in this study are represented in blue. Protein is depicted as palmitoylated and associated with membranes at the C-terminal palmitoylation site.

the plasma membrane could be due to increased transport of newly synthesized MLN-GFP-L^{15}L/AA from TGN to plasma membrane, although enhanced recycling of this mutant from endosomes to plasma membrane cannot be ruled out. Once at endosomes, transport to late endosomes and lysosomes could occur by default. Alternatively, extracellular or membrane-spanning domains could also participate in lysosomal sorting (31). The mutation of the internalization motif (MLN-GFP-L^{577}L/AA) did not cause accumulation at the plasma membrane, indicating that the protein can reach lysosomes through an exclusively intracellular or direct route. Although we cannot rule out the presence of additional internalization motifs at the N-terminal tail or within other intracellular loops, the complete block of the double mutant at the plasma membrane strongly argues against this possibility. Finally, the mutation of both di-leucine motifs (MLN-GFP-L^{15}L/AA-L^{577}L/AA) caused the delivery of the newly synthesized protein to the plasma membrane where it accumulated because it was unable to internalize.

In addition, we cannot discard the possibility that both N- and C-terminal di-leucines are acting as internalization motifs and that the different distribution of the Tac-MLN-NTail and Tac-MLN-CTail chimeras is a consequence of the N-terminal di-leucine being more efficient at mediating sorting at early endosomes. However, the failure to observe Tac-MLN-NTail at the plasma membrane in our BFA 'pulse–chase' and, more importantly, the lack of the accumulation of Tac-MLN-NTail at the plasma membrane in cells depleted of AP2 are more consistent with the hypothesis that the N-terminal di-leucine motif mediated direct transport from TGN to early endosomes (probably through interaction with AP1) and subsequent delivery from early endosomes to lysosomes (most likely due to interactions with AP3). Therefore, our results suggest that mucolipin-1 may use both direct and indirect routes to reach lysosomes.

It would be interesting to measure the fraction of newly synthesized mucolipin-1 that traffics via the plasma membrane. However, initial attempts by our laboratory to place a FLAG epitope at the first extracellular loop of mucolipin-1 or to detect biotinylated mucolipin-1 at the plasma membrane were unsuccessful. Nevertheless, the fact that MLN-GFP-L^{577}LAA does not significantly accumulate at the surface suggests that the direct route plays a major role in the sorting of mucolipin-1. Another possibility is that the internalization motif participates in alternative processes. For example, the exocytic fusion of lysosomes with the plasma membrane (32) could generate a pool of mucolipin-1 that should be quickly retrieved to lysosomes.

Palmitoylation is one of the most common post-translational modifications found in proteins and has been implicated in the regulation of membrane association, trafficking, protein–protein interaction and enzyme activity (33,34). Because of its reversibility, palmitoylation is a suitable mechanism to regulate the function of integral and peripheral membrane proteins. Treatment with palmitoylation inhibitors, mutation of specific cysteine residues and metabolic labeling with [^{3}H]palmitate led us to conclude that the C-terminal tail of mucolipin-1 is palmitoylated. The mutation of either of the cysteine residues in the sequence L^{564}CCC impaired the association of GFP-MLN-CTail with membranes, although the effect was more apparent when Cys566 was mutated to alanine. With the current data, we cannot determine whether all three cysteines are palmitoylated or whether the mutations of Cys565 and Cys567 affect the optimal palmitoylation of Cys566. It has recently been described that hydrophobic residues neighboring a cysteine can also influence palmitoylation. For example, the substitution of certain leucine residues with alanine abolishes palmitoylation of eNOS (35) and PSD95 (36). Consistently, the mutation of Leu564 to alanine also inhibited GFP-MLN-CTail palmitoylation, thus confirming the importance of residues adjacent to cysteines in the process.

Our data reveal that palmitoylation may be an important factor in the regulation of integral membrane protein endocytosis. Recently several groups have suggested that the internalization of a number of receptors such as CC chemokine receptor CCR5 (37), membrane-type matrix metalloproteinase-1 (38), and luteinizing hormone receptor (39) might also be regulated by palmitoylation. In the case of mucolipin-1, we propose that palmitoylation may promote internalization by bringing the C-terminal endocytosis motif closer to the plasma membrane, thus facilitating its interaction with AP2. Therefore, our results suggest that palmitoylation could regulate the efficiency of internalization of di-leucine motifs located at the end of long cytosolic tails. Finally, we cannot rule out the possibility that palmitoylation of mucolipin-1 has additional roles in regulating the traffic or

stability of the protein. For example, de-palmitoylation could make other determinants in the C-terminal tail accessible, promoting interactions with different effectors.

In conclusion, our data provide novel information toward understanding the intracellular pathways used by mucolipin-1 for targeting to lysosomes and emphasize the diversity of sorting mechanisms utilized in trafficking of lysosomal proteins.

Materials and Methods

Antibodies and reagents

The following antibodies were used: mouse monoclonal anti-EEA1 (BD Transduction Laboratories, San Jose, CA, USA), mouse monoclonal anti-CD63 (H5C6; Pharmingen, San Jose, CA, USA), mouse monoclonal anti-β subunit of AP2 (100/2; Sigma-Aldrich, St Louis, MO, USA), rabbit anti-GFP (MBL International, Woburn, MA, USA), mouse monoclonal anti-GFP (ab1218; Abcam, Cambridge, MA, USA), mouse monoclonal anti-IL2 Receptor alpha (Tac) (143–13; Abcam) and mouse monoclonal anti-annexin-II (Zymed, San Francisco, CA, USA). A polyclonal antibody to Hrs was the kind gift of S. Urbe (University of Liverpool, Liverpool, UK) (40). Mouse monoclonal anti-lamp-1 (Ac17) was obtained from E. Rodriguez-Boulan (Weill Medical College of Cornell University) (41).

Cycloheximide, 2-BP, leupeptin, BFA and protease inhibitor cocktail were obtained from Sigma (St Louis, MO, USA). Rhodamine-transferrin and Alexa555-EGF were supplied by Molecular Probes (Eugene, OR, USA). [^{3}H]Palmitate acid (30–60 Ci) was obtained from Perkin-Elmer (Boston, MA, USA).

Plasmids

The complete open reading frame of human mucolipin-1 was PCR amplified from a human brain cDNA library using specific primers and cloned into the pEGFP-N1 and pDs-Red-Monomer-N1 vectors (Clontech, Palo Alto, CA, USA). To generate the Tac chimeric constructs, we amplified the amino (amino acids 1–66) or carboxyl (amino acids 518–580) cytosolic tails of mucolipin-1 by PCR and cloned between an *Xba*I site inserted at the 3′ end of the Tac cDNA and the *Bam*HI site from the expression vector pCDL-SRα (42). The coding region of the Tac chimeras was then subcloned into the *Hind*III–*Bam*HI sites of the eukaryotic expression vector pcDNA3.1 (+) (Invitrogen, San Diego, CA, USA). The C-terminal cytosolic tail (amino acids 518–580) of mucolipin-1 was cloned into the *EcoR*I and *Sal*I sites of the pEGFP-C2 vector. Rab5-GFP and Rab5-GFP-Q79L are from R. Lodge (Laval, Quebec, Canada). AP2-GFP was obtained from L. Greene (National Institutes of Health, Bethesda, MD, USA) (43). Mutations of residues in the cytosolic tails of mucolipin-1 were introduced using the QUICKCHANGE site-directed mutagenesis kit (Stratagene, La Jolla, CA, USA).

SiRNA

RNAi of the μ2 subunit of the AP2 complex targeting the sequence GUGGAUGCUUUCGGGUCA was designed and synthesized as Option C by Dharmacon Research (Lafayette, CO, USA). Two consecutive transfections were carried out every 72 h in HeLa cells according to the manufacturer's instructions.

Transfection and immunofluorescence microscopy

The transfection of HeLa cells was performed using FuGENE-6 (Roche Molecular Biochemicals, Indianapolis, IN, USA). For immunofluorescence, transfected HeLa cells were grown on coverslips, fixed in methanol/acetone (1 : 1 v/v) for 10 min at −20 °C and subsequently air-dried. Incubation with primary antibodies diluted in phosphate-buffered saline (PBS), 0.1% (w/v) saponin, 0.1% bovine serum albumin (BSA), was carried out for 1 h at room temperature. Unbound antibodies were removed by rinsing with PBS for 5 min, and cells were subsequently incubated with a secondary antibody diluted in PBS, 0.1% (w/v) saponin, 0.1% BSA, for 30–60 min at room temperature. After a final rinse with PBS, coverslips were mounted onto glass slides with Fluoromount G (Southern Biotechnology Associates, Birmingham, AL, USA). Fluorescence images were acquired on an LSM 510 confocal microscope (Carl Zeiss, Thornwood, NY, USA).

To analyze trafficking of newly synthesized Tac chimeras, we transfected HeLa cells grown on coverslips with the corresponding cDNA for 6 h and then incubated with 2 μg/mL of BFA (Sigma-Aldrich) for 12 h to accumulate the newly synthesized proteins in the ER. The cells were then washed and incubated for different times at 37 °C in regular culture medium in the absence or presence of 20 μM leupeptin, fixed, permeabilized and analyzed by confocal microscopy.

Internalization assays

Internalization assays were carried out by incubation of transfected HeLa cells on ice for 1 h with an antibody against the extracellular domain of Tac diluted in PBS. The cells were washed extensively, incubated for 15 min at 37 °C in regular culture medium, fixed in methanol/acetone and incubated with a Cy3-conjugated anti-mouse IgG diluted in PBS, 0.1% (w/v) saponin, 0.1% BSA, for 30–60 min at room temperature. After a final rinse with PBS, coverslips were mounted onto glass slides with Fluoromount G (Southern Biotechnology Associates). Fluorescence images were acquired on an LSM 510 confocal microscope (Carl Zeiss).

Quantitative internalization assay

HeLa cells (1×10^6) were transiently transfected with the corresponding Tac chimera. Sixteen hours after transfection, cells were harvested in Cellstripper™ solution (Cellgro, Mediatech, Inc., Herndon, VA), washed once with cold PBS and incubated with anti-Tac antibody in PBS on ice for 60 min. After extensive washes, cells were split into two aliquots; one aliquot was directly fixed with 2% paraformaldehyde (time 0), and the other was incubated for 15 min at 37 °C, to allow cell-surface-bound antibodies to internalize before fixation. Cells were then stained with a fluorescein isothiocyanate-conjugated goat anti-mouse secondary for 30 min on ice, washed and analyzed by flow cytometry using a FACS-Calibur and CELLQUEST software (BD Biosciences, San Jose, CA, USA). Amounts of each chimeric protein remaining on the cell surface were defined as the specific fluorescence value, which was calculated after subtracting the mean fluorescence value of non-transfected cells from that of transfected cells. Percent internalization for each chimeric construct was calculated using the specific mean fluorescence value of cells fixed at time 0 as 100%. Results were expressed as the mean ± SD of at least three independent experiments. Measurements of forward scatter were used to exclude dead cells and debris.

Fractionation of HeLa cells and immunoblot

HeLa cells were transfected with GFP-MLN-CTail in the presence of ethanol (vehicle) or 50 mM of 2-BP and homogenized in HES buffer (20 mM Hepes, 250 mM sucrose, 1 mM EDTA, pH 7.4) supplemented with protease inhibitors. Postnuclear supernatants were separated by centrifugation at 196 000 × *g* for 60 min to yield cytosol (supernatant) and membranes (pellet) fractions.

Immunoblotting was carried out according to standard procedures. Proteins were separated by SDS-PAGE and transferred to nitrocellulose. The membrane was then blocked with PBS/0.05% Tween-20/10% dry milk and incubated with the indicated antibody. Enhanced chemiluminescence reagent (Amersham Bioscience, Piscataway, NJ, USA) was used for detection.

Metabolic labeling with [^{3}H]palmitic acid

Cells transfected with MLN-GFP or MLN-GFP-C^{565}CC/AAA for 24 h were washed twice with serum-free DMEM and labeled in 1.5 mL of DMEM containing 5% FBS, 20 mM Hepes pH 7.4 and 600 μCi of [^{3}H]palmitic acid for 6 h at 37 °C. Cells were then washed with ice-cold PBS and lysed in TNE buffer (25 mM Tris, 150 mM NaCl, 5 mM EDTA, 1% Triton-X-100, pH 7.4) supplemented with protease inhibitors. The lysate was precleared

by centrifugation and incubated with 5 μL of anti-GFP polyclonal antibody and protein G–Sepharose (Amersham Bioscience). Immunoprecipitates were collected, washed four times with PBS, eluted by incubation with Laemmli sample buffer for 10 min at room temperature and analyzed in two identical gels by SDS-PAGE under reducing conditions. One gel was fixed, treated with Amplify (Amersham Bioscience), dried and exposed to Kodak X-AR film for 15 days to visualize radiolabeled proteins, and the other gel was subjected to immunoblot analysis using the anti-GFP monoclonal antibody.

Acknowledgments

We thank Anitza San Miguel for excellent technical assistance and C. Mullins for critical reading of the manuscript. We also appreciate the editorial assistance of the NCI, CCR Fellows Editorial Board. This project was supported by the Intramural Research Program of the NIH, National Heart, Lung, and Blood Institute (NHLBI).

Supplementary Material

Figure S1. The C-terminal tail of mucolipin-1 does not co-localize with late endosomal–lysosomal markers. HeLa cells expressing Tac-MLN-CTail (red) were incubated with Alexa488-EGF for 10 min, washed and allowed to internalize for 2 h to load late endosomes (first row). The second row shows HeLa cells co-expressing Tac-MLN-CTail and Vamp7-GFP (lysosomal marker). Note that Tac-MLN-CTail has very little co-localization with both markers. Bar represents 10 μm.

Figure S2. The C-terminal tail of mucolipin-1 associates with intracellular membranes. HeLa cells were transfected with GFP-MLN-CTail either alone or in combination with the Tac-MLN-CTail chimera (fourth row). Transfected cells were fixed, permeabilized, immunostained with the indicated antibodies and examined by confocal fluorescence microscopy. For transferrin staining, cells were incubated with rhodamine-transferrin for 15 min at 37 °C. GFP-MLN-CTail is in green; transferrin, EEA1, Hrs and Tac-MLN-Tail are in red; yellow indicates co-localization. Bar represents 10 μm.

Figure S3. The Tac-MLN-NTail chimera does not reach the plasma membrane in its way to lysosomes. (A) HeLa cells treated with control (non-silencing) siRNA or siRNA targeted to the μ2 subunit of the AP2 complex were transfected with either Tac-MLN-CTail or Tac-MLN-NTail. Leupeptin (20 μM) was added 4 h before fixation of the cells, and the distribution of the chimeras was revealed by indirect immunofluorescence and confocal microscopy analysis. Bar represents 10 μm. (B) Quantification of cells treated with non-silencing siRNA or AP2 siRNA in which the corresponding chimera was localized mainly at the plasma membrane (PM) in the presence or absence of leupeptin. One hundred cells were counted for each condition.

Figure S4. Co-localization of mucolipin-1 wild-type and mucolipin-1 mutants with lysosomal markers. HeLa cells were transfected with MLN-GFP wild-type or the indicated mutants. Transfected cells were fixed, permeabilized, immunostained with an antibodies against lamp-1 and examined by confocal fluorescence microscopy. Yellow indicates co-localization. Bar represents 10 μm.

Figure S5. Role of palmitoylation in the trafficking of full-length mucolipin-1. HeLa cells were transfected with either MLN-GFP-L^{15}L/AA, in the presence of ethanol or the inhibitor of palmitoylation 2-bromopalmitate (2-BP) (upper panels), or with MLN-GFP carrying the C^{565}CC/AAA mutation alone or in combination with L^{15}L/AA (lower panels) and analyzed by confocal microscopy. Bar represents 10 μm.

These materials are available as part of the online article from http://www.blackwell-synergy.com

References

1. Bach G. Mucolipidosis type IV. Mol Genet Metab 2001;73:197–203.
2. Amir N, Zlotogora J, Bach G. Mucolipidosis type IV: clinical spectrum and natural history. Pediatrics 1987;79:953–959.
3. Altarescu G, Sun M, Moore DF, Smith JA, Wiggs EA, Solomon BI, Patronas NJ, Frei KP, Gupta S, Kaneski CR, Quarrell OW, Slaugenhaupt SA, Goldin E, Schiffmann R. The neurogenetics of mucolipidosis type IV. Neurology 2002;59:306–313.
4. Bargal R, Avidan N, Olender T, Ben Asher E, Zeigler M, Raas-Rothschild A, Frumkin A, Ben-Yosef O, Lancet D, Bach G. Mucolipidosis type IV: novel mutations in Jewish and non-Jewish patients and the frequency of the disease in the Ashkenazi Jewish population. Hum Mutat 2001;17:397–402.
5. Bach G, Cohen MM, Kohn G. Abnormal ganglioside accumulation in cultured fibroblasts from patients with mucolipidosis IV. Biochem Biophys Res Commun 1975;66:1483–1490.
6. Tellez-Nagel I, Rapin I, Iwamoto T, Johnson AA, Norton WT, Nitowsky H. Mucolipidosis IV: clinical, ultrastructural, histochemical and chemical studies of a case, including a brain biopsy. Arch Neurol 1976;33: 828–835.
7. Bach G, Zeigler M, Kohn G, Cohen MM. Mucopolysaccarides accumulation in cultured skin fibroblasts derived from patients with Mucolipidosis IV. Am J Hum Genet 1977;29:610–618.
8. Crandall BF, Philippart M, Brown WJ, Bluestone D. Mucolipidosis IV. Am J Med Genet 1982;12:301–308.
9. Folkerth RD, Alroy J, Lomakina I, Skutelsky E, Raghavan SS, Kolodny EH. Mucolipidosis IV: morphology and histochemistry of an autopsy case. J Neuropathol Exp Neurol 1995;54:154–164.
10. Chen CS, Bach G, Pagano RE. Abnormal transport along the lysosomal pathway in mucolipidosis, type IV disease. Proc Natl Acad Sci USA 1998;95:6373–6378.
11. Slaugenhaupt SA, Acierno JS, Hebing LA, Bove C, Goldin E, Bach G, Schiffmann R, Guesella JF. Mapping of the mucolipidosis type IV gene to chromosomal 19p and definition of founder haplotypes. Am J Hum Genet 1999;65:773–778.
12. Bargal R, Avidan N, Ben Asher E, Olender Z, Zeigler M, Frumkin A, Raas-Rothschild A, Glusman G, Lancet D, Bach G. Identification of the gene causing mucolipidosis type IV. Nat Genet 2000;26:118–123.
13. Bassi MT, Manzoni M, Monti E, Pizzo MT, Ballabio A, Borsani G. Cloning of the gene encoding a novel integral membrane protein mucolipin, and identification of the two major founder mutations causing mucolipidosis type IV. Am J Hum Genet 2000;67:1110–1120.
14. Sun M, Goldin E, Stahl S, Falardeau JL, Kennedy JC, Acierno JS, Bove C, Kaneski CR, Nagle J, Bromley MC, Colman M, Schiffmann R, Slaugenhaupt SA. Mucolipidosis type IV is caused by mutations in a gene encoding a novel transient receptor potential channel. Hum Mol Genet 2000;9:2471–2478.
15. Nilius B, Voets T, Peters J. TRP channels in disease. Sci STKE 2005;295: re8.
16. LaPlante JM, Falardeau J, Sun M, Kanazirska M, Brown EM, Slaugenhaupt SA, Vassilev PM. Identification and characterization of the single channel function of human mucolipin-1 implicated in mucolipidosis type IV, a disorder affecting the lysosomal pathway. FEBS Lett 2002;532:183–187.

17. Raychowdhury MK, Gonzalez-Perrett S, Montalbetti N, Timpanaro GA, Chasan B, Goldmann WH, Stahl S, Cooney A, Goldin E, Cantiello HF. Molecular pathophysiology of mucolipidosis type IV: pH dysregulation of the mucolipin-1 cation channel. Hum Mol Genet 2004;13:617–627.
18. Luzio JP, Poupon V, Lindsay MR, Mullock BM, Piper RC, Pryor PR. Membrane dynamics and the biogenesis of lysosomes. Mol Membr Biol 2003;20:141–154.
19. Fares H, Greenwald I. Regulation of endocytosis by CUP-5, the *Caenorhabditis elegans* mucolipin 1 homology. Nat Genet 2001;28: 64–68.
20. Hersh BM, Hartwieg E, Horvitz RH. The *Caenorhabditis elegans* mucolipin-like gene CUP-5 is essential for viability and regulates lysosomes in multiple cell types. Proc Nat Acad Sci USA 2002;99:4355–4360.
21. Treusch S, Knuth S, Slaugenhaupt SA, Goldin E, Grant BD, Fares H. *Caenorhabditis elegans* functional orthologue of human protein h-mucolipin-1 is required for lysosome biogenesis. Proc Natl Acad Sci USA 2004;101:4483–4488.
22. Marks MS, Roche PA, van Donselaar E, Woodruff L, Peters PJ, Bonifacino JS. A lysosomal targeting signal in the cytoplasmic tail of the beta chain directs HLA-DM to MHC class II compartments. J Cell Biol 1995;131:351–369.
23. Bonifacino JS, Traub LM. Signals for sorting of transmembrane proteins to endosomes and lysosomes. Annu Rev Biochem 2003;72: 395–447.
24. Webb Y, Hermida-Matsumoto L, Resh MD. Inhibition of protein palmitoylation, raft localization, and T cell signaling by 2-bromopalmitate and polyunsaturated fatty acids. J Biol Chem 2000;275:261–270.
25. Schweizer A, Kornfeld S, Rohrer J. Cysteine34 of the cytoplasmic tail of the cation-dependent mannose 6-phosphate receptor is reversibly palmitoylated and required for normal trafficking and lysosomal enzyme sorting. J Cell Biol 1996;132:577–584.
26. Manzoni M, Monti E, Bresciani R, Bozzato A, Barlati S, Bassi MT, Borsani G. Overexpression of wild-type and mutant mucolipin proteins in mammalian cells: effects on the late endocytic compartment organization. FEBS Lett 2004;567:219–224.
27. Janvier K, Bonifacino JS. Role of the endocytic machinery in the sorting of lysosome-associated membrane proteins. Mol Biol Cell 2005;16:4231–4242.
28. Lippincott-Schwartz J, Yuan LC, Bonifacino JS, Klausner RD. Rapid redistribution of Golgi proteins into the ER in cells treated with brefeldin A: evidence for membrane cycling from Golgi to ER. Cell 1989;56:801–813.
29. Li G, D'Souza-Schorey C, Barbieri MA, Roberts RL, Klippel A, Williams LT, Stahl PD. Evidence for phosphatidylinositol 3-kinase as a regulator of endocytosis via activation of Rab5. Proc Natl Acad Sci USA 1995;92:10207–10211.
30. Barbieri MA, Li G, Mayorga LS, Stahl PD. Characterization of Rab5:Q79L-stimulated endosome fusion. Arch Biochem Biophys 1996;326:64–72.
31. Reaves BJ, Banting G, Luzio JP. Lumenal and transmembrane domains play a role in sorting type I membrane proteins on endocytic pathways. Mol Biol Cell 1998;9:1107–1122.
32. Reddy A, Caler EV, Andrews NW. Plasma membrane repair is mediated by Ca(2+) -regulated exocytosis of lysosomes. Cell 2001;106:157–169.
33. Bijlmakers MJ, Marsh M. The on-off story of protein palmitoylation. Trends Cell Biol 2003;13:32–42.
34. Smotrys JE, Linder ME. Palmitoylation of intracellular signaling proteins: regulation and function. Annu Rev Biochem 2004;73: 559–587.
35. Liu J, Hughes TE, Sessa WC. The first 35 amino acids and fatty acylation sites determine the molecular targeting of endothelial nitric oxide synthase into the Golgi region of cells: a green fluorescent protein study. J Cell Biol 1997;137:1525–1535.
36. El-Husseini AE, Craven SE, Chetkovich DM, Firestein BL, Schnell E, Aoki C, Bredt DS. Dual palmitoylation of PSD-95 mediates its vesiculotubular sorting, postsynaptic targeting, and ion channel clustering. J Cell Biol 2000;148:159–172.
37. Kraft K, Olbrich H, Majoul I, Mack M, Proudfoot A, Oppermann M. Characterization of sequence determinants within the carboxyl-terminal domain of chemokine receptor CCR5 that regulate signaling and receptor internalization. J Biol Chem 2001;276:34408–34418.
38. Anilkumar N, Uekita T, Couchman JR, Nagase H, Seiki M, Itoh Y. Palmitoylation at Cys574 is essential for MT1-MMP to promote cell migration. FASEB J 2005;19:1326–1328.
39. Munshi UM, Clouser CL, Peegel H, Menon KM. Evidence that palmitoylation of carboxyl terminus cysteine residues of the human luteinizing hormone receptor regulates postendocytic processing. Mol Endocrinol 2005;19:749–758.
40. Sachse M, Urbe S, Oorschot V, Strous GJ, Klumperman J. Bilayered clathrin coats on endosomal vacuoles are involved in protein sorting toward lysosomes. Mol Biol Cell 2002;13:1313–1328.
41. Nabi IR, Le Bivic A, Fambrough D, Rodriguez-Boulan E. An endogenous MDCK lysosomal membrane glycoprotein is targeted basolaterally before delivery to lysosomes. J Cell Biol 1991;115:1573–1584.
42. Takebe Y, Seiki M, Fujisawa J, Hoy P, Yokota K, Arai K, Yoshida M, Arai N. SR alpha promoter: an efficient and versatile mammalian cDNA expression system composed of the simian virus 40 early promoter and the R-U5 segment of human T-cell leukemia virus type 1 long terminal repeat. Mol Cell Biol 1988;8:466–472.
43. Wu X, Zhao X, Puertollano R, Bonifacino JS, Eisenberg E, Green LE. Adaptor and clathrin exchange at the plasma membrane and trans-Golgi network. Mol Biol Cell 2003;14:516–528.